TABLE 5. Mean volume (%) of the rectal wall and bladder wall at endpoint doses of 20, 40, 60, and 70 Gy, according to the two multileaf collimators (MLCs).

	Rectal Wall			*Bladder Wall*		
Type of MLC	*m3*	*Millennium*	*p*	*m3*	*Millennium*	*p*
V20Gy (%)	80.1±6.3	80.7±6.1	< 0.01	34.7±13.2	35.5±13.7	0.02
V40Gy (%)	47.8±6.7	48.6±6.7	< 0.01	19.6±4.8	20.3±4.9	< 0.01
V60Gy (%)	21.6±5.1	22.2±5.2	< 0.01	11.7±2.7	12.1±2.7	< 0.01
V70Gy (%)	11.1±4.8	11.1±4.9	0.92	5.5±1.9	5.7±1.9	0.03

Values are expressed as the mean ± SD.

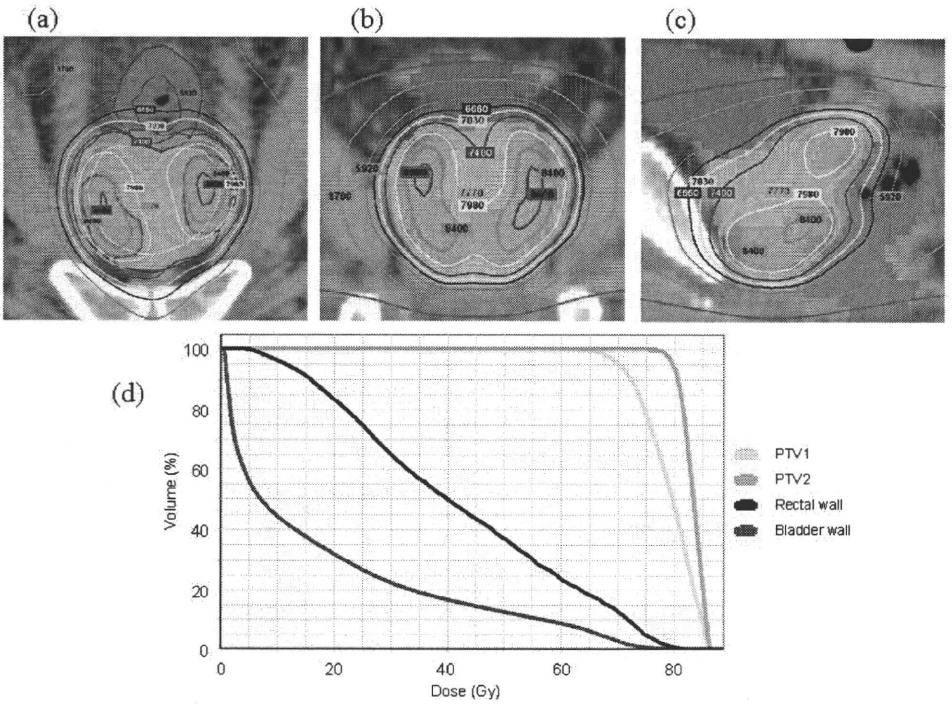

FIG. 3. Examples of the dose distribution of intraprostatic dose painting plan and dose volume histogram: (a) axial section; (b) coronal section; (c) saggital section; (d) dose-volume histogram.

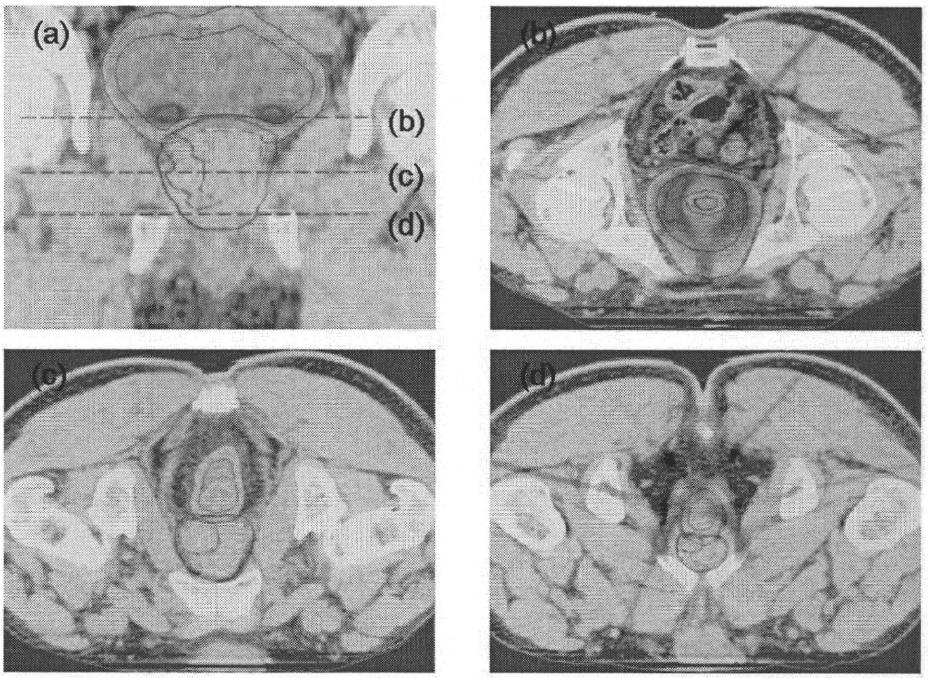

FIG. 4. Example of the difference in dose distribution between the m3 and Millennium plans for: (a) coronal section; (b) horizontal section at the level of the base of the prostate; (c) central region of the prostate; (d) apex of the prostate. The area displayed in color has a difference in dose distribution of > 2 Gy. The area displayed in red represents an area with a difference of > 5 Gy.

IV. DISCUSSION

The impact of MLC-W has been reported in several studies, and dosimetric advantages associated with thinner MLCs have been reported for stereotactic radiosurgery and IMRT, mainly in intracranial and head-and-neck cancer.[20, 22, 23] It is expected that MLC-W would also have an impact on dose distribution in the case of intraprostatic dose painting plans for prostate cancer because the doses to the relatively small targets within the prostate are intensified while retaining all dose constraints to the OARs. To our knowledge, there have been no reports regarding the impact of MLC-W on dose painting plans for localized prostate cancer using DMLC technique.

In IMRT treatment planning, it is difficult to simply compare different treatment units because of the large degree of freedom in dose delivery with the aid of computer optimization. Therefore, we set the same goals with respect to the targets and OARs, and repeated the optimization until all the goals were satisfied. In the present study, we set the goals that D95 was to be 95% (range 94.9%–95.1%) for both PTV1 and PTV2, and that the maximum dose to PTV2 was to be identical within ± 0.1 Gy among the different MLC plans. There were only very small differences in target coverage among the plans using the two different MLCs (Table 3 and Fig. 1). Therefore, a plan with a better conformity index is superior in this situation, because the target coverage is basically identical.

The maximum dose to the prostatic urethra was limited to < 82 Gy (Fig. 1). We did not set strict dose constraints for the rectal wall and bladder wall but limited the doses to the OARs in order to meet the dose-volume constraints that we currently apply in the clinical setting. Ideally, in comparing the CNs of two different MLCs, our plans should have included strict equivalent doses to the OARs. However, given the difficulty of achieving the dose constraints

set for PTV1, PTV2 and the prostatic urethra, it was unrealistic to set equivalent dose distributions to the OARs. Therefore, we set the dose constraints of the rectal wall and urinary bladder wall to meet the limits that we usually use in the clinic. The plan results show that the doses at the rectal wall were significantly lower for thinner MLCs, although the absolute values of the differences were small (Table 5).

The current study indicates that as MLC-W becomes thinner, the concentricity of the dose improves. However, differences in dose distribution between the m3 and Millennium plans were small. Regions with larger differences in dose distribution were located mainly in the superior and inferior borders of the fields (Fig. 4), which suggests that the MLC-W can put a direct impact on the dose distribution in the superior and inferior borders of the fields. On the other hand, only small differences were observed in the central part of the prostate, probably because the DMLC method provides for fine resolution of the dose steps along with the driving direction of the leaves. Therefore, if we were to use a multiple static field technique with fewer steps, the difference may become larger.

Only slight differences in the CNs were found among two different MLCs; thus the clinical influence of these differences is unclear. If these differences in conformality were to be spatially dispersed, the clinical impacts may be very small. Very small differences in dose distribution were found, as indicated in Fig. 4. This indicates that replacing a MLC of 5 mm width with one of 3 mm width has a relatively small clinical impact on dose distribution in intraprostatic dose painting plans using the DMLC technique for prostate cancer. Therefore, although a MLC of 3 -mm width can physically achieve a slightly better dose distribution, a MLC with a 5 mm width can also be used to achieve the expected dose distribution with this approach.

The volumes of PTV2 were smaller than those of PTV1 (Table 2). On comparing the CNs for PTV1 and PTV2, the CNs for PTV2 were consistently less than those for PTV1, which indicates that the concentricity would become poor. Because PTV2 was defined by adding a 5 mm margin to CTV2 as the DILs, it took various shapes in individual cases. Therefore, the concentricity may decrease if the shapes of PTV2 were intricate even if the volumes were identical. Hence, it may not be appropriate to determine the correlation of the CNs and the volumes of PTV with disregard to the shapes, especially for PTV2. A further study is necessary to consider a relation with the CNs.

The CNs for PTV1 and PTV2 were calculated with a calculation grid resolution of 1.25 × 1.25 mm, 2.5 × 2.5 mm and 5 × 5 mm (Table 4). Although there were differences in the CNs with different calculation grid size, the absolute values of the differences were small. In addition, the tendency of the difference between two MLCs was similar among three different calculation grid resolutions. Therefore, we consider that the impact of calculation grid size on the comparison of MLC-W was small, and hence, would not change clinical significance.

The results of the optimization are very much influenced by the optimization algorithm used in the radiotherapy treatment planning (RTP) system, and the results can vary when plans are created with other RTP systems. In addition, treatment machines and delivery techniques can have a large effect on the achievable dose distribution. Therefore, the results of this study may not be applicable to other RTP systems or treatment units.

In the clinical application of this approach, appropriate PTV to CTV (gross target volume) margins should be properly applied. In the present study, we used only a 5 mm margin to create PTV2. We believe that image-guided approaches such as implanted gold marker-based or CT-based error reductions should be used to ensure that the planned treatment doses are actually delivered.[28]

V. CONCLUSIONS

The planning goals set in the present intraprostatic dose painting planning protocol for localized prostate cancer were achieved using two different types of MLCs. However, dosimetric

advantages associated with smaller leaves were observed in terms of the conformity of the prescribed dose to the target, with a small but significant reduction in the rectal dose. When the DMLC technique is applied in this approach, a MLC with a 5 mm width may be sufficient, because any dosimetric disadvantage compared with a 3 mm-width MLC was relatively small.

ACKNOWLEDGEMENTS

This work was partially supported by Grants-in-Aid for Scientific Research from the Ministry of Education, Culture, Sports, Science, and Technology (20229009) and Grants-in-Aid for Scientific Research on Priority Areas Cancer from the Ministry of Education, Culture, Sports, Science, and Technology (17016036).

REFERENCES

1. Dearnaley DP, Sydes MR, Graham JD, et al. Escalated-dose versus standard-dose conformal radiotherapy in prostate cancer: first results from the MRC RT01 randomised controlled trial. Lancet Oncol. 2007;8(6):475–87.
2. Eade TN, Hanlon AL, Horwitz EM, Buyyounouski MK, Hanks GE, Pollack A. What dose of external-beam radiation is high enough for prostate cancer? Int J Radiat Oncol Biol Phys. 2007;68(3):682–89.
3. Kupelian PA, Mohan DS, Lyons J, Klein EA, Reddy CA. Higher than standard radiation doses (> or = 72 Gy) with or without androgen deprivation in the treatment of localized prostate cancer. Int J Radiat Oncol Biol Phys. 2000;46(3):567–74.
4. Peeters ST, Heemsbergen WD, Koper PC, et al. Dose-response in radiotherapy for localized prostate cancer: results of the Dutch multicenter randomized phase III trial comparing 68 Gy of radiotherapy with 78 Gy. J Clin Oncol. 2006;24(13):1990–96.
5. Pollack A, Zagars GK, Starkschall G, et al. Prostate cancer radiation dose response: results of the M. D. Anderson phase III randomized trial. Int J Radiat Oncol Biol Phys. 2002;53(5):1097–105.
6. Zelefsky MJ, Fuks Z, Hunt M, et al. High-dose intensity modulated radiation therapy for prostate cancer: early toxicity and biochemical outcome in 772 patients. Int J Radiat Oncol Biol Phys. 2002;53(5):1111–16.
7. Jackson A, Skwarchuk MW, Zelefsky MJ, et al. Late rectal bleeding after conformal radiotherapy of prostate cancer. II. Volume effects and dose-volume histograms. Int J Radiat Oncol Biol Phys. 2001;49(3):685–98.
8. Peeters ST, Heemsbergen WD, van Putten WL, et al. Acute and late complications after radiotherapy for prostate cancer: results of a multicenter randomized trial comparing 68 Gy to 78 Gy. Int J Radiat Oncol Biol Phys. 2005;61(4):1019–34.
9. De Meerleer GO, Fonteyne VH, Vakaet L, et al. Intensity-modulated radiation therapy for prostate cancer: late morbidity and results on biochemical control. Radiother Oncol. 2007;82(2):160–66.
10. Fenoglietto P, Laliberte B, Allaw A, et al. Persistently better treatment planning results of intensity-modulated (IMRT) over conformal radiotherapy (3D-CRT) in prostate cancer patients with significant variation of clinical target volume and/or organs-at-risk. Radiother Oncol. 2008;88(1):77–87.
11. Zelefsky MJ, Chan H, Hunt M, Yamada Y, Shippy AM, Amols H. Long-term outcome of high dose intensity modulated radiation therapy for patients with clinically localized prostate cancer. J Urol. 2006;176(4 Pt 1):1415–19.
12. Cahlon O, Zelefsky MJ, Shippy A, et al. Ultra-high dose (86.4 Gy) IMRT for localized prostate cancer: toxicity and biochemical outcomes. Int J Radiat Oncol Biol Phys. 2008;71(2):330–37.
13. Ling CC, Humm J, Larson S, et al. Towards multidimensional radiotherapy (MD-CRT): biological imaging and biological conformality. Int J Radiat Oncol Biol Phys. 2000;47(3):551–60.
14. Mohan R, Wu Q, Manning M, Schmidt-Ullrich R. Radiobiological considerations in the design of fractionation strategies for intensity-modulated radiation therapy of head and neck cancers. Int J Radiat Oncol Biol Phys. 2000;46(3):619–30.
15. Nutting CM, Corbishley CM, Sanchez-Nieto B, Cosgrove VP, Webb S, Dearnaley DP. Potential improvements in the therapeutic ratio of prostate cancer irradiation: dose escalation of pathologically identified tumour nodules using intensity modulated radiotherapy. Br J Radiol. 2002;75(890):151–61.
16. Pickett B, Vigneault E, Kurhanewicz J, Verhey L, Roach M. Static field intensity modulation to treat a dominant intra-prostatic lesion to 90 Gy compared to seven field 3-dimensional radiotherapy. Int J Radiat Oncol Biol Phys. 1999;44(4):921–29.
17. Singh AK, Guion P, Sears-Crouse N, et al. Simultaneous integrated boost of biopsy proven, MRI defined dominant intra-prostatic lesions to 95 Gray with IMRT: early results of a phase I NCI study. Radiat Oncol. 2007;2:36.
18. van Lin EN, Fütterer JJ, Heijmink SW, et al. IMRT boost dose planning on dominant intraprostatic lesions: gold marker-based three-dimensional fusion of CT with dynamic contrast-enhanced and 1H-spectroscopic MRI. Int J Radiat Oncol Biol Phys. 2006;65(1):291–303.
19. Xia P, Pickett B, Vigneault E, Verhey LJ, Roach M 3rd. Forward or inversely planned segmental multileaf collimator IMRT and sequential tomotherapy to treat multiple dominant intraprostatic lesions of prostate cancer to 90 Gy. Int J Radiat Oncol Biol Phys. 2001;51(1):244–54.

20. Fiveash JB, Murshed H, Duan J, et al. Effect of multileaf collimator leaf width on physical dose distributions in the treatment of CNS and head and neck neoplasms with intensity modulated radiation therapy. Med Phys. 2002;29(6):1116–19.
21. Jin JY, Yin FF, Ryu S, Ajlouni M, Kim JH. Dosimetric study using different leaf-width MLCs for treatment planning of dynamic conformal arcs and intensity-modulated radiosurgery. Med Phys. 2005;32(2):405–11.
22. Monk JE, Perks JR, Doughty D, Plowman PN. Comparison of a micro-multileaf collimator with a 5-mm-leaf-width collimator for intracranial stereotactic radiotherapy. Int J Radiat Oncol Biol Phys. 2003;57(5):1443–49.
23. Wang L, Hoban P, Paskalev K, et al. Dosimetric advantage and clinical implication of a micro-multileaf collimator in the treatment of prostate with intensity-modulated radiotherapy. Med Dosim. 2005;30(2):97–103.
24. Wu QJ, Wang Z, Kirkpatrick JP, et al. Impact of collimator leaf width and treatment technique on stereotactic radiosurgery and radiotherapy plans for intra- and extracranial lesions. Radiat Oncol. 2009;4(1):3.
25. Zhu S, Mizowaki T, Nagata Y, et al. Comparison of three radiotherapy treatment planning protocols of definitive external-beam radiation for localized prostate cancer. Int J Clin Oncol. 2005;10(6):398–404.
26. Mizowaki T, Cohen GN, Fung AY, Zaider M. Towards integrating functional imaging in the treatment of prostate cancer with radiation: the registration of the MR spectroscopy imaging to ultrasound/CT images and its implementation in treatment planning. Int J Radiat Oncol Biol Phys. 2002;54(5):1558–64.
27. van't Riet A, Mak AC, Moerland MA, Elders LH, van der Zee W. A conformation number to quantify the degree of conformality in brachytherapy and external beam irradiation: application to the prostate. Int J Radiat Oncol Biol Phys. 1997;37(3):731–36.
28. Schallenkamp JM, Herman MG, Kruse JJ, Pisansky TM. Prostate position relative to pelvic bony anatomy based on intraprostatic gold markers and electronic portal imaging. Int J Radiat Oncol Biol Phys. 2005;63(3):800–11.

Salvage Lung Resection for Non-small Cell Lung Cancer After Stereotactic Body Radiotherapy in Initially Operable Patients

Fengshi Chen, MD, PhD, Yukinori Matsuo, MD, PhD,† Akihiko Yoshizawa, MD, PhD,‡ Toshihiko Sato, MD, PhD,* Hiroaki Sakai, MD, PhD,* Toru Bando, MD, PhD,* Kenichi Okubo, MD, PhD,* Keiko Shibuya, MD, PhD,† and Hiroshi Date, MD, PhD**

Background: Stereotactic body radiotherapy (SBRT) has emerged as a curative treatment for medically inoperable patients with early-stage non-small cell lung cancer (NSCLC). Since NSCLC recurs locally in 10% of the patients treated with SBRT, salvage lung resection after SBRT may be considered in these cases. To further understand the indications for salvage surgery and the pathogenesis of tumor recurrence in these patients, we retrospectively reviewed cases treated at our institution.

Methods: SBRT has been performed in patients with early-stage NSCLC at Kyoto University Hospital. We encountered 5 patients who underwent salvage lung resection for NSCLC after SBRT.

Results: All the patients were initially operable, but they chose SBRT. After SBRT, the tumors shrank initially in all patients, but increased in size within 18 months of SBRT in the case of 4 patients. During surgical extirpation, we did not find any significant SBRT-related adhesions in any of the patients.

Conclusions: We have successfully treated 5 patients who underwent salvage lung resection for early-stage NSCLC after SBRT. We found that surgical resection was feasible after SBRT.

Key Words: Lung cancer, Lung resection, Recurrence, Salvage surgery, Stereotactic body radiotherapy.

(*J Thorac Oncol.* 2010;5: 1999–2002)

Stereotactic body radiotherapy (SBRT) is a recently developed radiotherapeutic method for early-stage non-small cell lung cancer, and failure of local control is estimated to occur in around 10% of the patients treated with SBRT. It has been reported that some patients develop local recurrence after SBRT and are then considered for salvage surgical resection.[1] In this study, we retrospectively reviewed five such cases treated at our institution to further understand the indications for salvage lung resection for non-small cell lung cancer after SBRT.

Departments of *Thoracic Surgery, †Radiation Oncology and Image-applied Therapy, and ‡Diagnostic Pathology, Kyoto University, Kyoto, Japan.

Disclosure: The authors declare no conflicts of interest.

Address for correspondence: Hiroshi Date, MD, Department of Thoracic Surgery, Kyoto University, 54 Shogoin-Kawahara-cho, Sakyo-ku, Kyoto 606-8507, Japan. E-mail: hdate@kuhp.kyoto-u.ac.jp

ISSN: 1556-0864/10/0512-1999

PATIENTS AND METHODS

Since 1998, three-dimensional conformal SBRT has been performed in patients with solitary lung tumors at the Kyoto University Hospital. The indications for SBRT have been already described elsewhere.[2,3] In short, the indications of SBRT in patients with lung cancer were as follows: (1) solitary tumor of less than 4 cm in diameter; (2) inoperable patients or patients refusing surgery; (3) performance status ≤2; and (4) a peripheral tumor in which dose constraints of mediastinal surrounding organs were maintained. During July 1998 and March 2008, SBRT was performed for 144 patients with primary lung cancer. Local recurrence was observed in 24 patients (16.7%) with a median follow-up of 31.5 months. Chemotherapy was administered for the local recurrence in nine patients including one patient with chemoradiotherapy. Best supportive care was chosen for 10 patients. Five patients were salvaged with surgery. Details on planning procedures were described in our previous article.[4] In summary, the internal target volume (ITV) was defined based on two imaging modalities: computed tomography (CT) with a slow-scan technique and x-ray fluoroscopy for evaluation of motion ranges of the tumor. When the ITV delineated on the slow-scan CT was insufficient to cover the tumor motion observed in the fluoroscopy, the ITV was manually expanded. The planning target volume for SBRT was set with a margin of 5 mm to the ITV. The total radiation dose was 48 Gy at the isocenter with a daily fractional dose of 12 Gy, except the initial three patients with 40 Gy. The irradiation was administered during a period of 1 to 2 weeks. The biologic effective dose was 105.6 Gy at the isocenter. The patients were followed up every 2 to 3 months after SBRT. When local recurrence was suspected from follow-up CT images, an fluorodeoxyglucose-positron emission tomography scan was performed, and radiology peer review was undertaken. If local recurrence without distant metastasis was considered highly probable on the basis of the review, the patient was referred to a thoracic surgeon for possible salvage resection. This study was approved by the institutional review board,

TABLE 1. Patient Characteristics at Stereotactic Body Radiotherapy (SBRT)

Patients	Age (yr)/ Gender	c-TNM Stage	Tumor Size (mm)	Histology	Reason for SBRT	Clinical Course After SBRT
1	63/M	T2N0M0	36	SQ	COPD (%FEV1 49%), DM, HD, and patient preference	Shrank but increased 10 mo after SBRT
2	75/M	T1N0M0	28	AD	COPD (%FEV1 57%), DM, angina, and patient preference	Shrank but increased 10 mo after SBRT
3	70/M	T1N0M0	24	Unknown	Patient preference	Shrank but increased 89 mo after SBRT
4	84/M	T1N0M0	19	AD or LCNEC	COPD (%FEV1 61%) and patient preference	Shrank but increased 8 mo after SBRT
5	75/M	T1N0M0	10	SQ	COPD (%FEV1 101%[a]) and patient preference	Shrank but increased 16 mo after SBRT

[a] $\%FEV_1$ was initially 77% at referral to our hospital, but finally increased up to 101% after intensive treatment with drugs and rehabilitation.

AD, adenocarcinoma; COPD, chronic obstructive pulmonary disease; DM, diabetes mellitus; HD, hemodialysis; LCNEC, large cell neuroendocrine carcinoma; M, male; NSCLC, non-small cell lung cancer; SQ, squamous cell carcinoma; SBRT, stereotactic body radiotherapy; %FEV1, percentage of forced expiratory volume in 1 s to a predicted value.

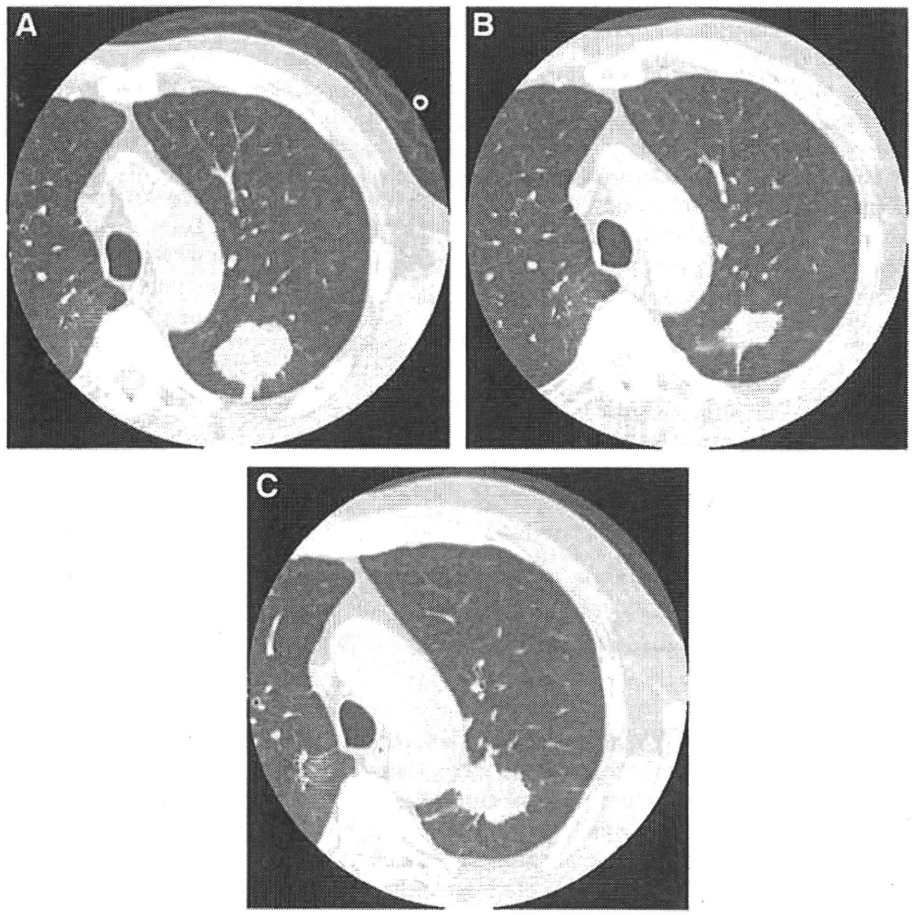

FIGURE 1. Clinical course of patient 1. *A*, Chest computed tomography (CT) at stereotactic body radiotherapy (SBRT) showed a mass with 36 mm in diameter in the left upper lobe. *B*, Chest CT 5 months after SBRT demonstrated remarkable tumor shrinkage. *C*, Chest CT 10 months after SBRT revealed an apparent tumor relapse.

and patient consent was waived because the study was retrospective and ensured anonymity.

RESULTS

In all the patients, a final decision for selecting SBRT was made as per the patient's preference (Table 1). Four patients had poor pulmonary functional reserve due to chronic obstructive pulmonary disease (COPD). According to GOLD classification of COPD, two patients were classified into stage IIa and one was stage IIb, whereas the rest patient, who had been initially classified stage I and had been referred to our hospital, became stage 0 after the medical treatment of COPD. After SBRT, the tumor shrank initially in all patients. The typical chest CT with clinical course was described in Figure 1. Continuous increase of the tumor in size is strongly indicative of tumor relapse after SBRT, although the patho-

TABLE 2. Patient Characteristics at Surgery

Patients	Interval between SBRT and Surgery	Surgical Procedure	yp-TNM Stage	Tumor Size (mm)	Histology	Outcomes
1	10 mo	Left upper lobectomy	T2N0M0	34	SQ	Alive for 25 mo
2	12 mo	Right upper lobectomy	T2N0M0	50	SQ	Alive for 31 mo
3	104 mo	Right upper lobectomy	T1N0M0	25	AD	Alive for 29 mo
4	17 mo	Left upper lobectomy	T2N0M0	33	LCNEC	Alive for 4 mo
5	21 mo	Right upper lobectomy	T1N0M0	28	SQ	Alive for 2 mo

AD, adenocarcinoma; LCNEC, large cell neuroendocrine carcinoma; SQ, squamous cell carcinoma; SBRT, stereotactic body radiotherapy.

logic diagnosis was not confirmed before surgical extirpation in all patients. At the time of recurrence, fluorodeoxyglucose-positron emission tomography scan revealed high uptake in the relapsed tumor in all patients. There were no apparent adverse complications related to SBRT in all five patients.

The preoperative condition of the patients was almost the same as that at the time of SBRT (Table 2). To be more specific, pulmonary function tests did not show any deterioration after SBRT in four patients who had COPD. In detail, the mean forced expiratory volume in 1 second (FEV_1) was 67% of the predicted value before SBRT in four patients with COPD, whereas FEV_1 was 73% of the predicted value before surgery. As salvage surgery, lobectomy with lymph node dissection was performed in all patients. Surgical extirpation did not confirm significant pleural adhesions in any patient. Furthermore, because there was no apparent SBRT-related change in the pulmonary structure, dissection around the vessels and bronchus was performed without difficulties. There were no complications during surgery, and postoperative course was also uncomplicated in all cases.

Histologically, three patients (patients 1, 2, and 5) were diagnosed as having squamous cell carcinoma. Patient 3, whose histologic subtype was not confirmed before SBRT, was diagnosed as having adenocarcinoma. Patient 4 was diagnosed as having large cell neuroendocrine carcinoma. All patients were pathologic stage I with a mean tumor size of 34 mm in diameter, ranging from 25 to 50 mm. The tumor size of four patients increased again within 18 months of SBRT. In three of the four patients (patients 1, 4, and 5), pathologic examination revealed that viable cancer cells were present in the center of the tumor with surrounding fibrotic tissue caused by SBRT (Figure 2). In one of the four patients (patient 2), microscopic findings showed central necrosis and viable cancer cells existed in the periphery of the tumor without surrounding fibrotic tissue caused by SBRT. In patient 3, microscopic findings showed that viable cancer cells were present in the center of the tumor, but one fifth of the circumference of the tumor was not surrounded by fibrotic tissue caused by SBRT.

The postoperative clinical course was uneventful in all patients. The median follow-up time was 27 months. All five patients are well, alive, and without any apparent tumor recurrences, including three patients who were followed up for more than 2 years after salvage surgery.

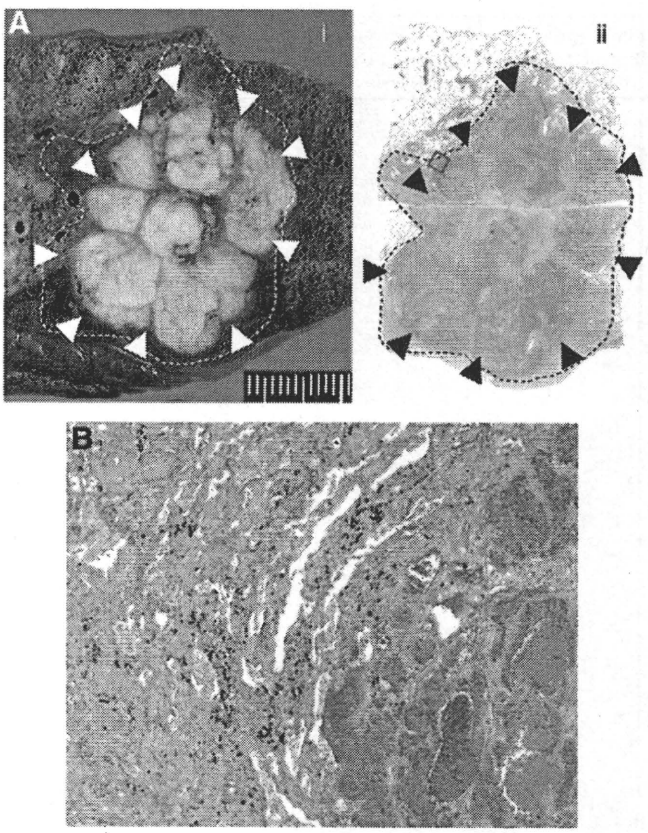

FIGURE 2. Pathologic findings (patient 1). *A*, (i) Cut surface of the resected lung after formalin fixation and (ii) loupe view showing a well-demarcated yellow-white nodular mass (arrowhead) in the center of fibrotic tissue caused by stereotactic body radiotherapy (SBRT) (dashed-line area). *B*, Microscopic appearance in the boundary area between a viable tumor nest (right lower area) and surrounding fibrotic tissue (left upper area). The field corresponds to the square in (*A*).

DISCUSSION

No adverse effect by SBRT was confirmed at the time of salvage surgery in our patients. Because the irradiated area was mainly confined to the peripheral lungs, central pulmonary structures such as the hilum were intact after irradiation. There was also almost no pleural adhesion related to the irradiation of the peripheral lung tissue including the tumor. It should be emphasized that surgery was performed without

complications, and postoperative course was also uncomplicated in all cases. Despite the small number of cases, we could for the first time confirm the points that most surgeons consider before performing surgical extirpation in such patients.

In this study, four patients relapsed within a relatively short time after SBRT. Considering that the tumor shrank after SBRT in these patients, SBRT had some effect on the tumor, but it is most likely that some residual tumor cells elapsed within a relatively short time after SBRT. To be more specific, in three of four patients whose tumor increased in size again within 18 months after SBRT, pathologic findings revealed viable cancer cells in the center of the tumor, surrounded by the fibrotic tissue caused by SBRT. These findings strongly suggested that the tumor relapsed in the central portion of the irradiated area, where the effect of SBRT theoretically tended to decrease because of the hypoxic environment of the tissue.[5,6] On the other hand, in one of four patients, microscopic examination of the tumor showed central necrosis and peripherally located viable cancer cell without surrounding tissue fibrosis caused by SBRT. These findings implied that dose to the tumor was insufficient at the center for the former three patients and at the periphery for the latter one. Two potential causes for the dose insufficiency were supposed: shortage in the planned dose and setup errors during the treatment. Optimization of dose prescription and setup correction are needed to improve local control after lung SBRT. The remaining one patient (patient 3) was unique in that the tumor relapsed very late after SBRT. Although the histologic diagnosis before SBRT was not obtained in this case, the second primary lung cancer, including radiation-induced carcinoma, might be more likely than recurrence of the primary lung cancer because of the relatively long disease-free period.[7] In this respect, long-term follow-up might be advised in this patient population, even beyond 5 years.

Serial measurements of the pulmonary function after SBRT also reportedly showed no significant decreases in several parameters including FEV1, as in this study.[8] In the current series, all five operable patients tolerated lung resection even after SBRT. Several randomized clinical trials comparing SBRT with surgery have been initiated,[9,10] and the results of these studies might pave the way to further understand SBRT as a method in the multimodality treatment. Despite a small number of cases, the findings of our study might be particularly relevant for these trials in operable patients. By contrast, the current low morbidity and mortality for lobectomy, especially video-assisted thoracoscopic lobectomy in elderly patients have enabled us to consider surgery confidently.[11] In this situation, the use of SBRT in patients who are medically fit for surgery should be decided more carefully.

REFERENCES

1. Haasbeek CJA, Lagerwaard FJ, Antonisse ME, et al. Stage I nonsmall cell lung cancer in patients aged ≥75 years. *Cancer* 2010;116:406–414.
2. Nagata Y, Negoro Y, Aoki T, et al. Clinical outcomes of 3D conformal hypofractionated single high-dose radiotherapy for one or two lung tumors using a stereotactic body frame. *Int J Radiation Oncol Biol Phys* 2002;52:1041–1046.
3. Nagata Y, Negoro Y, Aoki T, et al. Clinical outcomes of a phase I/II study of 48Gy of stereotactic body radiation therapy in four fractions using a stereotactic body frame. *Int J Radiat Oncol Biol Phys* 2005;63: 1427–1431.
4. Takayama K, Nagata Y, Negoro Y, et al. Treatment planning of stereotactic radiotherapy for solitary lung tumor. *Int J Radiat Oncol Biol Phys* 2005;61:1565–1571.
5. Rockwell S, Dobrucki IT, Kim EY, et al. Hypoxia and radiation therapy: past history, ongoing research, and future promise. *Curr Mol Med* 2009;9:442–458.
6. Karar J, Maity A. Modulating the tumor microenvironment to increase radiation responsiveness. *Cancer Biol Ther* 2009;8:1994–2001.
7. Zablotska LB, Neugut AI. Lung carcinoma after radiation therapy in women treated with lumpectomy or mastectomy for primary breast carcinoma. *Cancer* 2003;97:1404–1411.
8. Ohashi T, Takeda A, Shigematsu N, et al. Differences in pulmonary function before vs. 1 year after hypofractionated stereotactic radiotherapy for small peripheral lung tumors. *Int J Radiat Oncol Biol Phys* 2005;62:1003–1008.
9. Hurkmans CW, Cuijpers JP, Lagerwaard FJ, et al. Recommendations for implementing stereotactic radiotherapy in peripheral stage IA non-small cell lung cancer: report from the Quality Assurance Working Party of the randomized phase III ROSEL study. *Radiat Oncol* 2009;4:1.
10. Radiation Therapy Oncology Group (RTOG) 0618. A Phase II Trial of Stereotactic Body Radiation Therapy (SBRT) in the Treatment of Patients with Operable Stage I/II Non-Small Cell Lung Cancer. Available at: http://www.rtog.org/members/protocols/0618/0618.pdf. Accessed July 31, 2010.
11. Whitson BA, Groth SS, Duval SJ, et al. Surgery for early-stage non-small cell lung cancer: a systematic review of the video-assisted thoracoscopic surgery versus thoracotomy approaches to lobectomy. *Ann Thorac Surg* 2008;86:2008–2016.

JJCO Japanese Journal of Clinical Oncology

Jpn J Clin Oncol 2010;40(10)921–926
doi:10.1093/jjco/hyq077
Advance Access Publication 21 May 2010

Phase I/II Trial of Concurrent Use of S-1 and Radiation Therapy for T2 Glottic Cancer

Meijin Nakayama[1,*], Kazushige Hayakawa[2], Makito Okamoto[1], Yuzuru Niibe[2], Hiromichi Ishiyama[2] and Shouko Kotani[2]

[1]Department of Otorhinolaryngology, Kitasato University School of Medicine and [2]Department of Radiology, Kitasato University School of Medicine, Kanagawa, Japan

*For reprints and all correspondence: Meijin Nakayama, Department of Otorhinolaryngology, Kitasato University School of Medicine, 1-15-1 Kitasato, Sagamihara, Kanagawa 228-8555, Japan. E-mail: meijin@med.kitasato-u.ac.jp

Received March 8, 2010; accepted April 20, 2010

Objective: A Phase I/II study of S-1 combined radiation therapy was conducted in patients with Stage II (T2N0) glottic cancer. The purpose of the Phase I study was to identify the maximum tolerated dose, the recommended dose and the dose limiting toxicity. The objectives in the phase II study were to estimate the local control and the overall survival, and the incidence of adverse events.

Methods: In Phase I, S-1 was administered orally in a split-course fashion as two doses of 40 mg/m^2, for a total daily dose of 80 mg/m^2. The course involved a 2-week rest after a 2-week administration (Level 1) and a 1-week rest after a 3-week administration (Level 2). Radiation therapy was administered in 2-Gy daily (total 60-Gy) standard fractionation.

Results: Seven patients were enrolled in the Phase I, and 19 in the Phase II study. Mucositis was the most common toxicity encountered. All 26 patients completed radiation therapy without delay. The overall response rate was 100% (26/26) with all patients showing a complete response. One patient developed a local recurrence 28 months after the treatment. The 3-year local control and overall survival rates were 94.7 and 85.4%, respectively (limited to 22 patients from Level 2).

Conclusions: The use of S-1 at 80 mg/m^2 per day in a split-course with 1-week rest during the course of radiation therapy was safe and effective for Stage II glottic cancer. The treatment strategy employing orally available S-1 proved to be beneficial over the conventional injection of antitumor agents for maintaining the patients' quality of life.

Key words: laryngeal cancer – chemoradiation – S-1 – Phase I – Phase II study

INTRODUCTION

Laryngeal cancer is one of the head and neck malignancies with good prognosis. Several clinical factors contribute to the good prognosis, including the high proportion of patients diagnosed at early stages of diseases, the efficacy of chemoradiation, and the diversity of available surgical options. Radiation therapy (RT) plays a major role in the treatment of laryngeal cancer and is particularly effective with regard to laryngeal preservation. In addition, the landmark RTOG 91-11 trial provided evidence of the clinical significance of combining chemotherapy with RT (1). Various chemotherapeutic agents have been reported to be effective for head and neck cancers, although selecting an appropriate dose and administration schedule for combination with RT can be difficult. S-1, a novel orally available combination of tegafur, gimeracil and oteracil potassium at a 1:0.4:1 molar ratio, is effective for the treatment of head and neck cancers (2–5). Although gimeracil displays no antitumor activity, it suppresses the metabolism and deactivation of 5-fluorouracil (FU) in the body, thus increasing the radiosensitivity of tumors (6).

Herein, we report the results of a Phase I/II study of S-1 combined with RT in patients with squamous cell carcinoma of the larynx. The purpose of the Phase I study was to

identify the maximum tolerated dose (MTD), the recommended dose (RD) and the dose limiting toxicity (DLT). The primary objectives of the Phase II study were to estimate the local control rate and the overall survival rate, and the secondary objectives were to assess the overall response rate and incidence of adverse events.

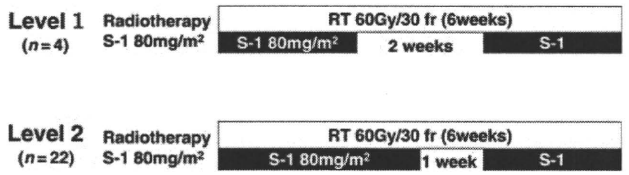

Figure 1. Plan for the combined use of S-1 with radiation therapy (RT) for treatment of laryngeal cancer.

PATIENTS AND METHODS

Eligibility Criteria

The eligibility criteria were: (i) the presence of histologically confirmed glottic squamous cell carcinoma; (ii) the identification of carcinoma as Stage II disease (T2N0); (iii) no previous treatment history (primary case); (iv) the presence of measurable lesions; (v) no history of RT to the head and neck regions; (vi) age between 20 and 80 years; (vii) a performance status of 0–1 on the Eastern Cooperative Oncology Group (ECOG) scale; (viii) a life expectancy $\geq$3 months; (ix) ability to receive drugs orally; (x) provision of written informed consent; and (xi) adequate bone marrow, liver and kidney functions, which were determined by (a) leukocyte count 4000/mm^3 less than or equal to $<$12 000/mm^3, (b) platelet count $\geq$100 000/mm^3, (c) hemoglobin $\geq$9.0 g/dl, (d) aspartate aminotransferase (AST), alanine aminotransferase (ALT) $<$100 U/l, (e) All $P \leq 2$ times the upper limit of the normal value, (f) total bilirubin $\leq$1.5 mg/dl and (g) serum creatinine $<$ the upper limit of the normal value.

Exclusion Criteria

The exclusion criteria were: (i) the presence of any active concomitant malignancies; (ii) serious complications, including (a) active infectious disease, diarrhea, intestinitis, pancreatitis, paralytic enterocolitis, ileus, interstitial pneumonitis, pulmonary fibrosis, (b) uncontrolled massive pleural effusion or ascites, (c) gastrointestinal bleeding, (d) uncontrolled diabetes mellitus or (e) cardiac failure, renal failure, liver dysfunction, etc.; (iii) uncontrolled angina pectoris or myocardial infarction within the previous 3 months; (5) active gastro-duodenal ulcer; (v) severe neuropathy; (vi) pregnancy or plans to become pregnant; (vii) a male patient with plans to impregnate; (viii) a past history of severe allergic reaction to drugs; or (ix) ineligibility as determined by the study physicians.

Treatment Plan: Dosage and Drug Escalation

During Phase I, S-1 (formulated by Taiho Pharmaceutical Co., Tokyo, Japan) was administered orally in a split-course fashion as two doses of 40 mg/m^2 for, a total daily dose of 80 mg/m^2. The course involved a 2-week rest after a 2-week administration (Level 1) and a 1-week rest after a 3-week administration (Level 2; Fig. 1). Level 3 was not established based upon the prescribed instructions for S-1. The duration of S-1 administration was increased in a stepwise fashion for both levels of the study.

In Phase II, patients received the RD of S-1 combined with RT. S-1 was withheld for the following toxicities: (i) leukocyte count $<$2000/mm^3; (ii) platelet count $<$100 000/mm^3; (iii) diarrhea Grade 3 or higher; (iv) mucositis Grade 3 or higher. Treatment resumed after recovery to the baseline. If patients did not recover from these toxicities within 28 days of the last administration of S-1, they were withdrawn from the study. If any of the severe toxicities was observed, then the dose of S-1 was reduced by 20 mg per day.

Radiotherapy

Radiotherapy was administered in 2-Gy daily standard fractions using 4 MV X-rays. The total dose of radiation was fixed at 60-Gy. Patients were treated in the supine position under a plastic shell. Two parallel-opposed lateral fields were used with a pair of wedge filters (Fig. 2). A computed

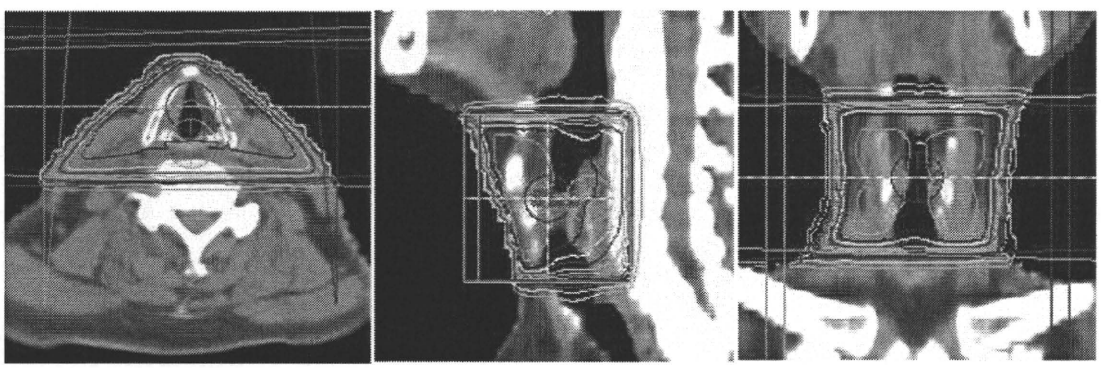

Figure 2. Administration of RT. A colour version of this figure is available as supplementary data at http://www.jjco.oxfordjournals.org.

tomography-based treatment-planning system was mandatory to define the planned target volume.

RT was withheld for the following toxicities: (i) leukocyte count $<1500/mm^3$; (ii) platelet count $<50\,000/mm^3$; or (iii) mucositis Grade 3 or higher. Radiation was resumed after recovery to baseline. Termination of the treatment course following Grade 3 mucositis was dependent upon the patient's condition and the physician's judgment.

MTD, RD and Sample Size

In the Phase I study, the MTD was defined as the dose level that produced DLT in at least two of three patients or least three of six patients (If DLT occurred in one or two of the first three patients, three additional patients were assigned to receive the same dose level). If none of the three patients initially receiving a given dose level displayed DLT, or if only one or two out of six patients had DLT, the dose was increased to the next level. If the Level 1 dose was not acceptable, this regimen would not be considered feasible and then the study would be stopped.

DLT was defined by the following parameters: (i) Grade 4 hematologic toxicity; (ii) fever (body temperature $\geq 38°C$) with Grade 3 neutropenia; or (iii) Grade 3/4 thrombocytopenia or Grade 3/4 non-hematologic toxicity (including radiation induced mucositis) except for nausea and vomiting. DLT was evaluated on the basis of adverse events occurring within 1 week after the completion of chemoradiotherapy.

The sample size was increased for the Phase II study because this study was designed to detect an expected CR rate of 70% (the threshold over 40%) with a power of 90% with a statistical significance level of 0.05 ($\alpha = 0.05$, $\beta = 0.1$). The required sample size was 21 patients at the RD, including those treated at the RD during the Phase I. However, an additional four patients were included in order to accommodate potential losses due to ineligibility, drop-outs or major protocol violations.

Outcome Measure

Drug-related adverse events were classified according to the National Cancer Institute Common Toxicity Criteria (NCI-CTC) version-2 (7). Hematological and biochemical tests were performed at least every week, and the patient performance status and clinical symptoms were assessed every day. The tumor response was evaluated according to the Response Evaluation Criteria in Solid Tumors (RECIST) criteria (8). Assessments by imaging studies were repeated every 4 weeks during the study. Local control was defined as the time from registration until the earliest documented time to death, disease progression or salvage surgery at the primary site. Overall survival was defined as the time from registration until death from any cause (censored at the time of the last visit in patients who were lost to follow-up). The local control rate and overall survival rate were estimated using the Kaplan–Meier method. To evaluate the effect of single dose intensity, data of 22 patients from Level 2 were used for overall survival and local control analyses.

Ethical Consideration

This study was conducted in accordance with the principles of the Declaration of Helsinki and Good Clinical Practice guidelines. The protocol for this Phase I/II trial was approved by the Institutional Review Board of Kitasato University Hospital. All patients provided their written informed consent before study entry.

RESULTS

Patient Characteristics

A total of 26 patients were enrolled in this study at the Departments of Otolaryngology and Radiology at Kitasato University Hospital between January 2003 and May 2007. Seven patients (four patients in Level 1 and three patients in Level 2) were enrolled in the Phase I study and 19 patients in the Phase II study. The clinical data for the 26 patients enrolled in the trial is listed in Table 1. Twenty-five males and one female with a median age of 66 years (range 53–80) were treated. All 26 patients had glottic cancers staged as T2N0. Among the 26 patients, 15 (58%) and 11 (42%) were classified as favorable and unfavorable T2, respectively, according to the clinical guideline proposed by American Society of Clinical Oncology (ASCO) (9).

Toxicity

None of the four patients enrolled at Level 1 developed DLT. In Level 2, none of the initial three patients developed DLT. From these results, the RD was determined to be Level 2. The treatment-related adverse events (most severe grade reported during the treatment period) are tabulated in Table 2. Mucositis was the most common adverse event, and was observed in 4, 17 and 5 patients at Grade 1, 2 and 3, respectively. Most of the patients were able to eat a soft diet and complete the treatment course in an out patient setting. Three patients from Level 2 (one patient with G-3 and two with G-2 mucositis) required nasogastric alimentation in an inpatient setting in the middle of the treatment course.

Of the 22 patients who received the RD of S-1, only one patient (#22 displayed as 3W-1X-2X in Table 1) discontinued the administration of S-1 after the break due to the development G-2 mucositis and G-2 renal dysfunction. One patient (#7) with G-1 liver dysfunction was given a reduced dose of S-1 after the break. No patients aged 76–80 years old experienced any severe toxicity. In addition, all patients completed RT without delay.

Response

The overall response rate was 100% (26/26) with all patients showing complete response. The 3-year local control and

Table 1. Clinical data of the 26 patients enrolled for Phase I/II trial

#	Enroll	Gender	Age	T2	S-1	Response	Mucositis	Admission	Follow (m)	Prognosis
1	2003	M	78	Favorable	2W-2X-2W	CR	G1	–	81	Alive and well
2	2003	M	72	Favorable	2W-2X-2W	CR	G1	–	78	Alive and well
3	2003	F	57	Unfavorable	2W-2X-2W	CR	G2	–	77	Alive and well
4	2003	M	67	Unfavorable	2W-2X-2W	CR	G2	–	77	Alive and well
1	2003	M	59	Favorable	3W-1X-2W	CR	G2	O	72	Alive and well
2	2003	M	68	Favorable	3W-1X-2W	CR	G2	–	76	Alive and well
3	2003	M	64	Favorable	3W-1X-2W	CR	G2	–	72	Alive and well
4	2003	M	64	Favorable	3W-1X-2W	CR	G2	–	29	Died of Lung Ca
5	2004	M	55	Favorable	3W-1X-2W	CR	G3	–	62	Alive and well
6	2004	M	80	Unfavorable	3W-1X-2W	CR	G1	–	6	Lost to follow up
7	2004	M	60	Favorable	3W-1X-2W	CR	G2	–	69	Alive and well
8	2004	M	65	Favorable	3W-1X-2W	CR	G2	–	33	Died of Lung Ca
9	2005	M	62	Favorable	3W-1X-2W	CR	G2	–	62	Alive and well
10	2005	M	62	Unfavorable	3W-1X-2W	CR	G2	–	56	Alive and well
11	2005	M	65	Unfavorable	3W-1X-2W	CR	G2	–	47	Alive and well
12	2005	M	68	Favorable	3W-1X-2W	CR	G2	–	55	Alive and well
13	2005	M	53	Unfavorable	3W-1X-2W	CR	G2	–	38	Alive and well
14	2006	M	64	Unfavorable	3W-1X-2W	CR	G1	–	51	Alive and well
15	2006	M	69	Unfavorable	3W-1X-2W	CR	G2	O	49	Alive and well
16	2006	M	63	Favorable	3W-1X-2W	CR	G2	–	43	Alive and well
17	2006	M	65	Unfavorable	3W-1X-2W	CR	G3	O	41	Alive and well
18	2006	M	76	Favorable	3W-1X-2W	CR	G3	–	43	Alive and well
19	2006	M	72	Favorable	3W-1X-2W	CR	G3	–	21	Died of dist met
20	2006	M	76	Unfavorable	3W-1X-2W	CR	G2	–	39	Alive and well
21	2007	M	73	Favorable	3W-1X-2W	CR	G3	–	36	Alive and well
22	2007	M	62	Unfavorable	3W-1X-2X	CR	G2	O	36	Recurred/salvaged

O, yes for admission.

overall survival rates were 94.7 and 85.4%, respectively, in the 22 patients from Level II (Fig. 3).

One patient (#22) developed a local recurrence 28 months after the completion of S-1 combined RT and was subsequently salvaged by a supracricoid laryngectomy with cricohyoidoepiglottopexy (SCL-CHEP). One patient (#19) died from lung metastasis without local recurrence. Two patients (#4 and #8) died from primary lung cancers. One patient was lost to follow-up 6 months after the completion of treatment course.

DISCUSSION

Laryngeal preservation is one of the main objectives for the management of laryngeal cancer. In 2006, ASCO proposed clinical practice guidelines for the use of laryngeal preservation strategies (9). The guidelines advocate that all patients with T1 or T2 cancer should be initially treated with the intent to preserve the larynx. In addition, an approach that preserves the larynx should also be considered for most patients with T3 or T4 disease. Concurrent chemoradiotherapy plays a major role in the management of laryngeal preservation. The ASCO guidelines also recommended that T2 laryngeal cancer should be classified as either favorable T2 (a superficial tumor with normal cord mobility) or unfavorable T2 (a deeply invasive tumor, subglottic extension and impaired cord mobility). In unfavorable T2 cases, chemoradiation therapy and open organ preservation surgery should be considered rather than using RT alone. This is especially important in light of the fact that deep invasion and impaired cord mobility are major prognostic factor for radiation failure (10).

Concurrent chemoradiation therapy with oral antitumor agents is an easy and patient-oriented treatment option for

Table 2. Treatment-related adverse events for the 26 patients (indicated as the most severe grade reported during the treatment period)

Toxicity	Phase 1 ($n = 4$)						Phase 2 ($n = 22$)					
	Grade					≥ G3 (%)	Grade					≥ G3 (%)
	0	1	2	3	4		0	1	2	3	4	
Hematologic												
Leukopenia	4	0	0	0	0	0	18	4	0	0	0	0
Neutropenia	4	0	0	0	0	0	20	2	0	0	0	0
Anemia	4	0	0	0	0	0	21	1	0	0	0	0
Thrombocytopenia	4	0	0	0	0	0	18	4	0	0	0	0
ALT	4	0	0	0	0	0	20	2	0	0	0	0
AST	4	0	0	0	0	0	18	4	0	0	0	0
Total bilirubin	4	0	0	0	0	0	21	1	0	0	0	0
Creatinine	4	0	0	0	0	0	21	0	1	0	0	0
Non-hematologic												
Mucositis	0	2	2	0	0	0	0	2	15	5	0	23
Anorexia	4	0	0	0	0	0	16	2	4	0	0	0
Nausea	4	0	0	0	0	0	21	0	1	0	0	0
Diarrhea	4	0	0	0	0	0	18	3	1	0	0	0
Fatigue	4	0	0	0	0	0	17	1	4	0	0	0
Pigmentation	4	0	0	0	0	0	20	2	0	0	0	0

Toxicity classified according to NCI-CTC version 2.0. AST: aspartate aminotransferase; ALT: alanine aminotransferase.

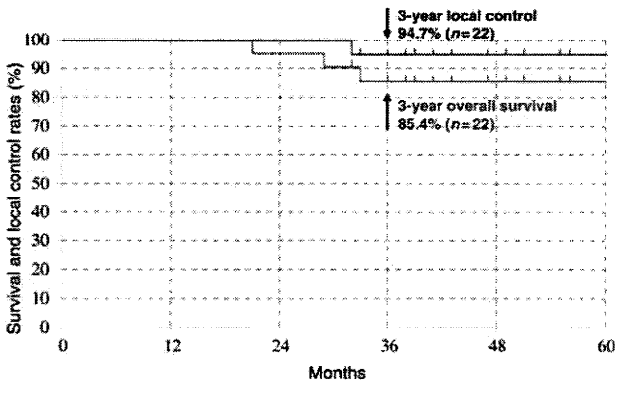

Figure 3. Three-year local control and overall survival rates were evaluated using the Kaplan–Meier method. A colour version of this figure is available as supplementary data at http://www.jjco.oxfordjournals.org.

early stage laryngeal cancer. A previous study reported that uracil–tegafur (UFT) combined with RT is effective in treating early stage laryngeal cancer (11). The authors observed no severe adverse reactions with this treatment regimen. Niibe et al. (2) confirmed the high local control rate of UFT combined RT and mentioned the potential use of S-1, a novel orally available combination of agent derived from UFT.

S-1 (Taiho Pharmaceutical Co., Ltd) is orally available combination of tegafur (a prodrug converted to 5-FU), gimeracil (an inhibitor of dihydropyrimidine dehydrogenase, which is responsible for 5-FU catabolism) and oteracil potassium (an inhibitor of phosphorylation of 5-FU in the gastrointestinal tract). The combination of agents is designed to enhance the anticancer activity and reduce the gastrointestinal toxicity of fluoropyrimidine therapy (12). A Phase II trial of advanced and recurrent SCCHN (59 eligible cases) showed a high response rate of 28.8% with acceptable toxicities (13).

In the current Phase I/II trial, only one patient (#22) experienced a local recurrence and this was detected 28 months after the completion of the treatment. Since S-1 was discontinued after the break due to G-2 renal dysfunction in this patient, the local recurrence may have been associated with the modification of S-1 administration. None of the other patients developed a local recurrence during the follow-up time of 6–81 months (median 52 months). The high rate of local control in this trial was superior to the initial expectations, particularly when considers the number of unfavorable T2 patients included in the study. Although, the antitumor effect of S-1 greatly contributed to the improved outcome for patients, it is also likely that S-1 sensitized the tumor to radiotherapy. The radiosensitizing effect of S-1 has been reported by several investigators. For example, Harada et al. (5) reported that S-1 increases the *in vivo* radioresponse of tumor xenografts derived from oral cancer cells; furthermore, the authors reported that 5-FU sensitizes the *in vitro* radioresponse of these cells by suppressing the activation of Akt/PKB, an important survival signal. Employing nude mice bearing hypopharyngeal cancer cell (H891), as an *in vivo* model, Nakagawa et al. (14) demonstrated that S-1 had an additive antitumor effect when combined with RT.

Although a randomized trial comparing combined S-1/RT and RT alone in head and neck cancers is still unavailable, combined 5-FU/RT has been reported to impart better therapeutic effects than RT alone (15). The radiosensitizing effect of 5-FU strongly depends on the continuous exposure of the targeted cancers to 5-FU following irradiation (16). The pharmacokinetic feature of S-1 fits well in maintaining effective level for prolonged tumor exposure.

In this study, G-3 mucositis occurred in 28% (7/25) of the patients receiving RD. This was higher than that in a recent study of CCRT for glottic cancer (3). The difference is likely related to the higher dose of S-1 used in the current study. Symptoms of mucositis can be managed with analgesics and mouthwash. Even though four patients in our study required a modification of S-1 administration, all 29 patients in the trial completed RT without delay. Since, Hayakawa et al. (17) reported that prolongation of the radiation schedule adversely affected local control of T1 glottic carcinoma, it appears that it is beneficial to combine S-1 with RT, since the addition of S-1 did not increase host toxicity due to RT. Thus, chemoradiation with S-1 and RT (60-Gy) seems to be a feasible and effective combined regimen for treating early to moderate stage laryngeal cancer.

It is also important to mention that proper maintenance of high quality RT, including a strict distribution pattern and

overall treatment time, is imperative (18). Results may vary depending on the quality of RT facilities and staff. In addition, the potential use of supracricoid laryngectomy (SCL), an open laryngeal preservation surgery, may have influenced the proper case selection in this trial. SCL is offered as an alternative treatment option along with S-1/RT, particularly for the treatment of patients with unfavorable T2 and T3 status. A previous study demonstrated that SCL is beneficial for the treatment of T2 and T3 cases (19). However, patients with favorable T2 status might be curable by RT alone. Further investigations are needed to establish the clinical indicators for proper case allocation among RT, S-1/RT and laryngeal preservation surgeries.

CONCLUSION

The use of S-1 at 80 mg/m^2 per day in a split-course with 1-week rest during the course of RT was safe and effective for Stage II glottic cancer. The treatment strategy employing orally available S-1 proved to be beneficial over the conventional injection of antitumor agents for maintaining the patients' quality of life.

Acknowledgements

This study was presented at the 50th Annual Meeting of American Society for Radiation Oncology (ASTRO 2008 in Boston). The authors thank M. Uemae RT and associates for maintaining consistently high quality for the daily radiation therapy. The authors declare that there are no conflicts of interest in this study.

Conflict of interest statement

None declared.

References

1. Forastiere A, Goepfert H, Maor M, Pajak T, Weber R, Morrison W, et al. Concurrent chemotherapy and radiotherapy for organ preservation in advanced laryngeal cancer. *N Engl J Med* 2003;349:2091–8.
2. Niibe Y, Nakayama M, Matsubayashi T, Takahashi H, Kitano M, Okamoto M, et al. Effectiveness of concurrent radiation therapy with UFT or TS-1 for T2N0 glottic cancer in Japan. *Anticancer Res* 2007;27:3497–500.
3. Tsuji H, Kiba T, Nagato M, Inoue T, Yukawa H, Yamashita T, et al. A phase I study of concurrent chemoradiotherapy with S-1 for T2N0 glottic carcinoma. *Oncology* 2006;71:369–73.
4. Choi Y, Chung J, Shin H-J, CHO G, Wang S, Lee B, et al. Induction chemotherapy with S-1 plus cisplatin in patients with locally advanced squamous cell carcinoma of the head and neck. *J Laryngol Otol* 2008;122:848–53.
5. Tsukuda M, Ishitoya J, Mikami Y, Matsuda Y, Horiuchi C, Taguchi T, et al. Analysis of feasibility and toxicity of concurrent chemoradiotherapy with S-1 for locally advanced squamous cell carcinoma of the head and neck in elderly cases and/or cases with comorbility. *Cancer Chemother Pharmacol* 2009;64:945–52.
6. Harada K, Kawaguchi S, Suprianto, Onoue T, Yoshida H, Sato M. Combined effects of the oral fluoropyrimidine anticancer agent, S-1 and radiation on human oral cancer cells. *Oral Oncology* 2004;40:713–9.
7. National Cancer Institute: National Cancer Institute Common Toxicity Criterior (version 2). Bethesda: Division of Cancer Treatment and Diagnosis, National Cancer Institute 1999.
8. Therasse P, Arbuck S, Eisenhauer E, Wander J, Kaplan R, Rubinstein L, et al. New guidelines to evaluate the resonse to treat in solid tumors. European Organization for Research and Treatment of Cancer, National Cancer Institute of the United States, National Cancer Institute of Canada. *J Natl Cancer Inst* 2000;92:205–16.
9. Pfister D, Laurie S, Weinstein G, Mendenhall W, Adelstein D, Kian Ang K, et al. American society of clinical oncology clinical practice guideline for the use of larynxpreservation strategies in the treatment of laryngeal cancer. *J Clin Oncol* 2006;24:3693–704.
10. Harwood A, Deboer G. Prognostic factors in T2 glottic cancer. *Cancer* 1980;45:991–5.
11. Takahashi H, Yao K, Sawaki S, Kubota A, Tsukuda M, Miyake H, et al. Investigation on UFT radiation therapy on head and neck cancer—mainly in laryngeal cancer. *Jpn J Cancer Chemother* 1990;17:2037–42.
12. Shirasaka T, Nakano K, Takechi T, Satake H, Uchida J, Fujioka A, et al. Antitumor activity of 1M tegafur-0.4 M 5-chloro-2, 4-dihydoxypyridine-1M potassium oxonate (S-1) against human colon carcinoma orthotopically implanted into nude rats. *Cancer Res* 1996;56:2602–6.
13. Inuyama Y, Kida A, Tsukuda M. Late phase II study of S-1 in patients with advanced head and neck cancer. *Gan To Kagaku Ryoho* 2001;28:1381–90.
14. Nakagawa T, Otsuki N, Masai Y, Sasaki R, Tsukuda M, Nibu K. Additive effects of oral fluoropyrimidine derivative S-1 and radiation on human hypopharyngeal cancer xenografts. *Acta Otolaryngol* 2008;128:936–40.
15. Lo T, Wiley A, Ansfield F, Brandenburg J, Davis H, Gollin F, et al. Combined radiation therapy and 5-fluorouracil for advanced squamous cell carcinoma of the oral cavity and oropharynx: a randomized study. *Am J Roentgenol* 1976;126:229–35.
16. Smalley S, Kimler B, Evans R. 5-Fluorouracil modulation of radiosensitivity in cultured human carcinoma cells. *Int J Radiat Oncol Biol Phys* 1991;20:207–11.
17. Hayakawa K, Mitsuhashi N, Akimoto T, Maebashi K, Ishikawa H, Hayakawa k, et al. The effect of overall treatment time of radiation therapy on local control of T1-Stage squamous cell carcinoma of the glottis. *Laryngoscope* 1996;106:1545–7.
18. Kitano M, Nishiguchi I, Aoki Y, Nakayama M, Nagai H, Takahashi H, et al. Relation between overall treatment time and local control of early glottic cancer: comparison of six versus five times per week. *Nippon Acta Radiologica* 2002;62:366–9.
19. Nakayama M, Okamoto M, Miyamoto S, Yokobori S, Takeda M, Masaki T, et al. Supracricoid laryngectomy with cricohyoidoepiglottopexy or cricohyoido-pexy: Experience on 32 atients. *Auris Nasus Larynx* 2008;35:77–82.

Radiol Phys Technol
DOI 10.1007/s12194-010-0084-z

Evaluation of the usefulness of a MOSFET detector in an anthropomorphic phantom for 6-MV photon beam

Ryosuke Kohno · Eriko Hirano · Satoshi Kitou · Tomonori Goka · Kana Matsubara · Satoru Kameoka · Taeko Matsuura · Takaki Ariji · Teiji Nishio · Mitsuhiko Kawashima · Takashi Ogino

Received: 23 July 2009 / Revised: 7 January 2010 / Accepted: 8 January 2010

Abstract In order to evaluate the usefulness of a metal oxide-silicon field-effect transistor (MOSFET) detector as a in vivo dosimeter, we performed in vivo dosimetry using the MOSFET detector with an anthropomorphic phantom. We used the RANDO phantom as an anthropomorphic phantom, and dose measurements were carried out in the abdominal, thoracic, and head and neck regions for simple square field sizes of 10 × 10, 5 × 5, and 3 × 3 cm^2 with a 6-MV photon beam. The dose measured by the MOSFET detector was verified by the dose calculations of the superposition (SP) algorithm in the XiO radiotherapy treatment-planning system. In most cases, the measured doses agreed with the results of the SP algorithm within ±3%. Our results demonstrated the utility of the MOSFET detector for in vivo dosimetry even in the presence of clinical tissue inhomogeneities.

Keywords MOSFET detector · In vivo dosimetry · Anthropomorphic phantom · Inhomogeneity · Superposition algorithm

R. Kohno (✉) · E. Hirano · S. Kitou · T. Goka · S. Kameoka · T. Matsuura · T. Ariji · T. Nishio · M. Kawashima · T. Ogino
National Cancer Center Hospital East, 6-5-1 Kashiwanoha, Kashiwa, Chiba 277-8577, Japan
e-mail: rkohno@east.ncc.go.jp

R. Kohno
National Cancer Center Research Institute, 5-1-1 Tsukiji, Chuo-ku, Tokyo 104-0045, Japan

K. Matsubara
Graduate School of Human Health Sciences, Tokyo Metropolitan University, 7-2-10 Higashiogu, Arakawa-ku, Tokyo 116-8551, Japan

T. Matsuura
Foundation for Promotion of Cancer Research, 5-1-1 Tsukiji, Chuo-ku, Tokyo 104-0045, Japan

T. Nishio
Graduate School of Medicine, University of Tokyo, 7-3-1 Hongo, Bunkyo-ku, Tokyo 113-8655, Japan

Published online: 04 February 2010

1 Introduction

For implementation of radiation therapy with high-energy photon beams in the clinics, comprehensive dose verifications are essential. Generally, dose verifications on phantoms are recommended and carried out for each irradiation condition [1–4]. However, this does not mean that these verifications assure a perfect actual radiation dose to the patients. On the other hand, in vivo dosimetry can be used to identify major deviations in the delivery of treatment. Thus, we regard in vivo dosimetry during patient treatment as the ultimate dose verification for patient quality assurance (QA). Here, in order to carry out in vivo dosimetry, the detector must be very small, and easy to localize. To achieve this goal, we used metal oxide-silicon field-effect transistor (MOSFET) detectors (Best Medical Canada, Ottawa, Canada).

The MOSFET detector has a very small sensitive volume, which is a 0.2 mm × 0.2 mm, 0.5-μm-thick layer of insulating of silicon dioxide. The detector which we used is a dual-MOSFET detector consisting of two identical MOSFETs fabricated on the same silicon chip and operating at two different gate bias voltages, allowing temperature compensation of the detector response [5]. The MOSFET detector has been widely used for measuring radiation doses [6–11], and the accuracy, reliability, and usefulness of the MOSFET detector in clinical applications such as pinpoint absolute dosimetry has been reported [12].

An accurate estimate of the radiation dose is important for verifying that the expected dose of radiation has been delivered to the patient. Chuang et al. used a MOSFET detector in intensity-modulated radiation therapy (IMRT) dosimetric verification for routine IMRT phantoms, a solid water slab phantom, and a cylindrical PMMA phantom [7]. These dose verifications were performed on homogeneous materials. Carrasco et al. [13] measured percentage depth doses in inhomogeneous-layer phantoms containing water- and bone-equivalent materials using a MOSFET detector. The MOSFET detector was found suitable for dose measurement inside bone-equivalent materials. On the other hand, MOSFET detectors have previously been employed in surface dose measurements during in vivo dosimetry [8, 12, 14]. However, these measurements were not performed under the variable conditions created by inhomogeneous specimens containing water-, lung-, and bone-equivalent materials.

Here, we evaluated dose measurements using the MOSFET detector in inhomogeneous regular slab phantoms, as shown in "Appendix". The dose verification results for the superposition (SP) algorithm with use of the MOSFET detectors were similar to Kohno's results with use of the Farmer ionization chamber [15]. In general, the degree of accuracy in the dose measurement with MOSFET detectors is not as high as that with ionization chambers. However, we demonstrated that the MOSFET detector can measure doses with sufficient accuracy for various tissue-equivalent phantoms, various regular geometries, and various field sizes. From a different point of view, we can also say that it is important to measure dose independently using detectors with different characteristics, in order to evaluate the results of dose measurements in difficult irradiation conditions such as the presence of inhomogeneities.

On the other hand, the human body does not have a simple geometry such as the above regular slabs, and it forms complex inhomogeneities with bone, soft tissue, various materials, and various shapes. Therefore, it may not be certain that the results of dose verifications for slab-based phantoms can be extrapolated to actual clinical cases. In this paper, to evaluate the usefulness of the MOSFET detector as an in vivo dosimeter under more realistic conditions, we performed in vivo dosimetry using an anthropomorphic phantom.

2 Materials and methods

2.1 Experimental apparatus

Experiments were carried out with a Siemens ONCOR linear accelerator (Siemens Medical Solutions USA, Concord, CA) with a dual-focus, multi-leaf collimator. The specified uncertainty of the leaf positions was ±1 mm. For dose measurements, we used TN-502RD MOSFET detectors and the mobileMOSFET reader, set at the standard bias sensitivity. The MOSFET and a calibrated 0.6 cc Farmer ionization chamber type 30013 (PTW, Freiburg, Germany) were placed in a dose calibration phantom made of PMMA. Tough Water phantoms manufactured by Kyoto Kagaku Co., Ltd (Kyoto, Japan) were stacked on the dose calibration phantom. With a 6-MV photon beam at a dose rate of 300 MU/min, a dose of 100 MU was delivered at 100 cm source-to-axis distance (SAD), at a depth of 10 cm within a field of 10×10 cm^2 for calibration of the MOSFET response.

Measurements were carried out for simple square field sizes of 10×10, 5×5, and 3×3 cm^2 with a 6-MV photon beam. All measurement points were set in the center of an exposed square area. We used a beam angle of 0° for all of the experiments, thus avoiding uncertainties (~2%) of angular dependence [7, 11] of the MOSFET detector in the dose measurements, and unnecessary complexities in the SP dose calculations. We estimated the reproducibility as ±1.5% (1 standard deviation) for five consecutive irradiations of 100 MU each.

2.2 Anthropomorphic phantom

The RANDO anthropomorphic phantom (The Phantom Laboratory, Salem, CA) [16] provides a detailed mapping of the dose distribution that is essential for evaluating radiotherapy treatment plans. RANDO phantoms are constructed with a natural human skeleton cast inside a material that is radiologically equivalent to soft tissue. The RANDO lungs are molded to fit the contours of the natural human rib cage. The properties of the RANDO materials are listed in Table 1. The ρ_{nominal} value is the nominal electron density relative to water for tissue-equivalent materials. Physical densities and effective atomic numbers of the tissue-equivalent materials are also shown in Table 1. The MOSFET detectors were placed within cavities in the phantom.

First, the detector positions were selected in the abdominal region. As shown in Fig. 1a and b, the abdominal region in the phantom is homogeneous. The measurement point is indicated by a cross mark, and the measurement depths for Fig. 1a and b were 6 and 9.5 cm, respectively.

Next, the dose measurement points for the chest region are illustrated in Fig. 2a–c. Figure 2a depicts a region of the mediastinum, which is a soft tissue. This measurement point is at an interface of the mediastinum and lung, with the beam central axis in the interface. On the other hand, Fig. 2b and c is in the lung region, and thus we were able to

Table 1 Electron densities relative to water obtained by CT number conversion (ρ_{meas}), effective atomic number, and physical densities of the tissue-equivalent materials in the RANDO phantom used in this study

Phantom	Soft tissue	Lung
$\rho_{nominal}$	0.979	0.311
ρ_{meas}	1.014 ± 0.003	0.231 ± 0.015
Effective atomic number	7.60	7.11
Physical density (g/cm^3)	0.997	0.352

$\rho_{nominal}$ nominal electron density relative to water

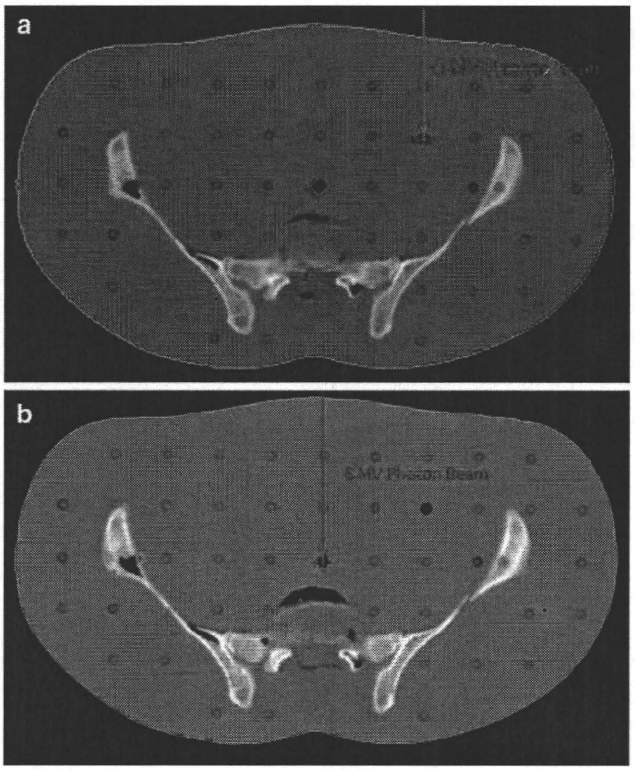

Fig. 1 The homogeneous abdominal region of the anthropomorphic phantom. The measurement point is indicated by a *cross mark*, and the measurement depths for **a** and **b** were 6 and 9.5 cm, respectively. Measurements were carried out for simple square field sizes of 10 × 10, 5 × 5, and 3 × 3 cm^2 and a beam angle of 0° with a 6-MV photon beam. All measured points were set in the center of an exposed square area

evaluate the dose for low-density material. The measurement depths for Fig. 2b and c were 4.5 and 7.5 cm, respectively.

Figure 3a, b, and c illustrates measurement locations in the head and neck region. In Fig. 3a, the dosimeter is located at the center of the posterior arch of the first cervical vertebra in the RANDO phantom. The dose here was formed by the photon beam passing through the jaw, consisting of cortical bone, and the oral cavity, consisting of air. Figure 3b is the location posterior to the sella in the RANDO phantom, which corresponds to the surface of the brainstem. This region also consists of bone, cavities, and soft tissue, and forms complex inhomogeneities. Because of the presence of many critical structures, it is important to deliver accurate doses in this region. Figure 3c is a location posterolateral to the posterior arch of the first cervical vertebra.

2.3 Dose calculation and data analysis

The XiO 4.33.02 radiotherapy planning (RTP) system for dose calculations was used in this study. Doses were calculated using SP algorithm [17] with inhomogeneity correction. Here, the Monte Carlo (MC) method as a dose calculation algorithm is a powerful tool for analytic calculations and for verification of results obtained in difficult measurements situations. However, because the MC has considerable difficulties and uncertainties in reconstructive techniques based on measured depth dose distributions for clinical photon beams [18], we did not use it in this study. On the other hand, the SP has already been verified for various irradiation conditions by many authors [15, 17–21, "Appendix"] and has been widely adopted in clinical use. Therefore, using the SP as a dose calculation algorithm is reasonable for comparing the calculation dose with the MOSFET dose in this study. Three-dimensional dose distributions were calculated with 0.2 cm resolution.

Phantom information was obtained from computed tomography (CT) images. The CT images of all phantoms were acquired with an Asteion (Toshiba Medical Systems Corp., Tokyo, Japan) CT scanner at a 2.5 mm slice thickness and 2.5 mm slice separation. The electron density of each tissue, ρ_{meas}, is obtained by CT number conversion, and we used this value obtained by CT scan in our dose calculations. Here, the ρ_{meas} of the lung material in Table 1 was somewhat smaller than the $\rho_{nominal}$. We assume that the lung material of the RANDO phantom changed over time. This may have led to overestimates in the dose calculations.

Dosimetric magnitudes were analyzed in terms of absolute doses. D_{calc} is the calculated dose at a measurement point in the phantom, and D_{meas} is the measured dose at the same point. The dose measured at each point was compared to the calculated dose, and the discrepancy at the measurement point, $\delta(\%)$, was evaluated as a percentage of the measured dose:

$$\delta(\%) = \frac{D_{calc} - D_{meas}}{D_{meas}} \times 100.$$

The error bars in each figure represent the reproducibility of the MOSFET dose.

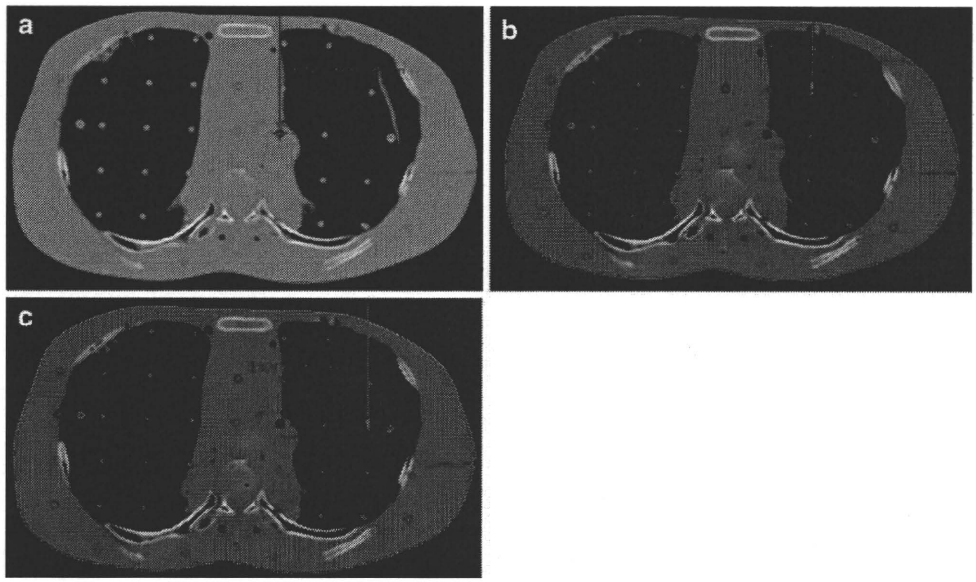

Fig. 2 The chest region of the anthropomorphic phantom. The *cross marks* represent the measurement point. **a** A region of the mediastinum. **b** and **c** The lung region. The measurement depths for **b** and **c** were 4.5 and 7.5 cm, respectively. Measurements were carried out for simple square field sizes of 10 × 10, 5 × 5, and 3 × 3 cm^2 and a beam angle of 0° with a 6-MV photon beam. All measured points were set in the center of an exposed square area

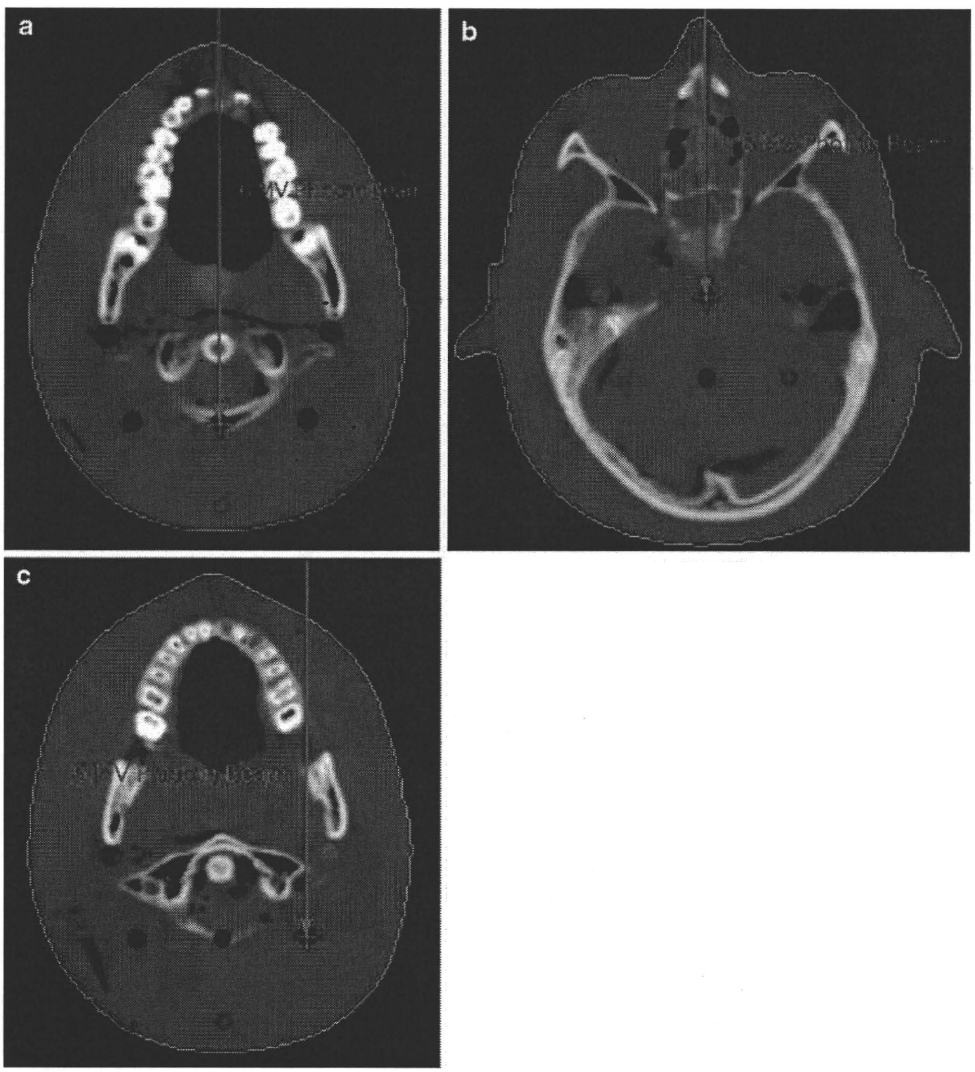

Fig. 3 The head and neck region of the anthropomorphic phantom. The *cross marks* represent the measurement point. **a** The dosimeter is located at the center of the posterior arch of the first cervical vertebra in the RANDO phantom. **b** The location posterior to the sella in the RANDO phantom. **c** A location posterolateral to the posterior arch of the first cervical vertebra. Measurements were carried out for simple square field sizes of 10 × 10, 5 × 5, and 3 × 3 cm^2 and a beam angle of 0° with a 6-MV photon beam. All measured points were set in the center of an exposed square area

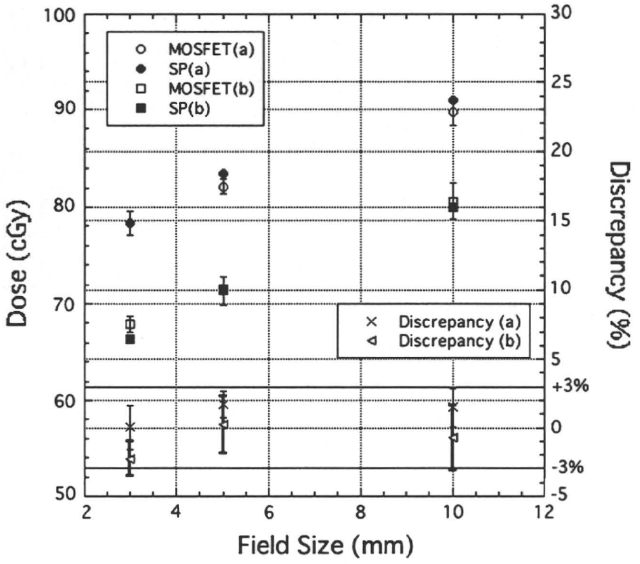

Fig. 4 Comparisons between the doses measured with the MOSFET detector and doses calculated by use of the SP algorithm for the homogeneous abdominal region of Fig. 1. The measurement depths for **a** and **b** were 6 and 9.5 cm, respectively. This figure also includes the discrepancy (%) between doses measured with the MOSFET detector and doses calculated with the SP algorithm

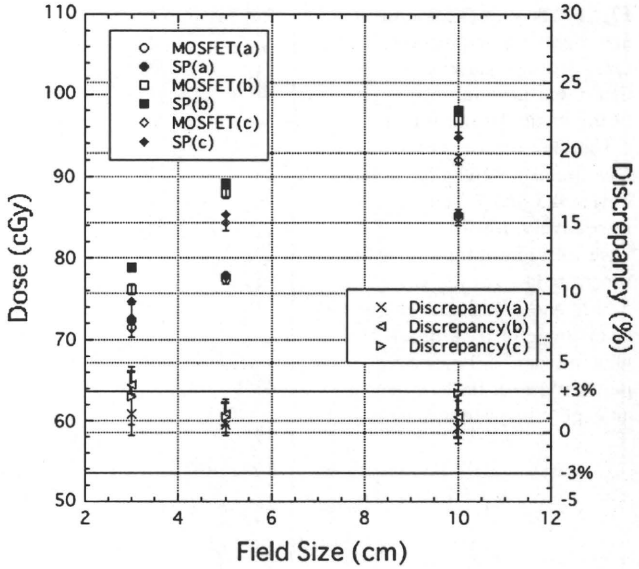

Fig. 5 Comparisons between the doses measured with the MOSFET detector and doses calculated by use of the SP algorithm for the chest region of Fig. 2. Evaluation point (Fig. 2**a**) is a region of the mediastinum, and **b** and **c** are in the lung region. The measurement depths for Figs 2**b** and **c** were 4.5 and 7.5 cm, respectively. This figure also includes the discrepancy (%) between doses measured with the MOSFET detector and doses calculated with the SP algorithm

3 Results and discussion

Figure 4 contains comparisons between doses measured with the MOSFET detector and doses calculated by the SP method for soft tissue for Fig. 1a and b, respectively. This figure also includes the discrepancy (%) between doses measured with the MOSFET detector and doses calculated with the SP algorithm. The measured doses agreed with the results of the SP algorithm within ±3%.

Comparisons between the measurements and calculations for the chest region (Fig. 2a–c) are displayed in Fig. 5. We observed that the SP overestimates the dose particularly in the lung region (Fig. 2b, c) compared with the measurements. We can explain this by an underestimation by use of the relative electron density for lung material, as shown in Table 1. Then, the difference of the doses between MOSFET and SP at a field size of 3 cm is larger than those at 5 and 10 cm. Because the leaf position uncertainty of ±1 mm contributes approximately 0.5% to the dose uncertainty for the 3 × 3 cm^2 field size, it may be one of the causes of the larger difference.

Figure 6 depicts comparisons between doses measured with the MOSFET detector and doses calculated with the SP algorithm for the head and neck measurements mapped in Fig 3a–c. Here, Kohno et al. [15] reported that a definite deterioration in the dose prediction accuracy occurred when they used the SP algorithm in bone material for a field size of 3 × 3 cm^2. Moreover, Fig. 8c also supported the deterioration. Therefore, the SP algorithm would display significant differences in Fig. 3a due to the inadequate energy deposition kernel model for bone material [19]. However, even in this complex inhomogeneous region, the measured doses agreed with the results of the SP algorithm within ±3%. We concluded that the actual body does not include large and thick bones such as this in Fig. 7c, which results in a large deterioration of the dose prediction due to the incomplete energy deposition kernel model in the photon dose calculation.

Thus, dose measurements by use of the MOSFET detector were compared with calculations by the SP algorithm for various irradiation conditions. The small size, immediate read-out, and fast response of the MOSFET detector make it particularly useful for dose measurements for therapeutic MV photon beams. The results of our dosimetric measurements demonstrate the utility of the MOSFET detector for clinical dosimetry in radiotherapy. Our dose measurements were performed at a beam angle of 0°. Given the variety of beam angles used in actual radiotherapy, the ±2% angular dependence of the MOSFET detector must be considered [7, 11]. The angular dependence may lead to a decrease in accuracy at some angles, which, in turn, may affect the clinical utility of this detector.

4 Conclusion

We evaluated in vivo dosimetry with a MOSFET detector for an anthropomorphic phantom. Dose measurements